Original Article

# Oxidative phosphorylation-related genes for prognosis and tumor microenvironment in breast cancer

**Man-Zhi Xia, Shu-Feng Dong, Chun-Lei Wang**

Department of General Surgery, Shaoxing Maternity and Child Health Care Hospital, Shaoxing, China

*Contributions:* (I) Conception and design: MZ Xia; (II) Administrative support: MZ Xia; (III) Provision of study materials or patients: CL Wang; (IV) Collection and assembly of data: MZ Xia, SF Dong; (V) Data analysis and interpretation: MZ Xia, CL Wang; (VI) Manuscript writing: All authors; (VII) Final approval of manuscript: All authors.

*Correspondence to:* Chun-Lei Wang, MD. Department of General Surgery, Shaoxing Maternity and Child Health Care Hospital, Fenglin East Road 222, Yuechen District, Shaoxing 312000, China. Email: wangchunlei72@163.com.

**Background:** Oxidative phosphorylation (OXPHOS) is a major energy resource occurring in mitochondria. Targeting OXPHOS-related genes has emerged as potential targets for cancer therapy. This study aimed to explore the significance of OXPHOS-related genes in breast cancer (BRCA).

**Methods:** Differentially expressed genes (DEGs) related to OXPHOS in BRCA were identified using packages of Limma and VennDiagram using the data from public databases. A prognostic model based on differentially expressed OXPHOS-related genes was constructed using least absolute shrinkage and selection operator Cox regression analyses and then evaluated through Kaplan-Meier and receiver operator characteristic (ROC) curves. Additionally, gene set variate analysis (GSVA) and gene set enrichment analysis (GSEA) were performed to explore the potential pathways involved in BRCA. Furthermore, the tumor microenvironment (TME) difference between low- and high-risk BRCA groups was investigated. The prognostic significance of hub genes was then examined. We conducted a protein-protein interaction (PPI) network to uncover the potential gene interactions and identify key genes, whose expressions were validated in cells.

**Results:** Our analyses revealed 234 differentially expressed OXPHOS-related genes, from which a nine-gene (*ATP5PF*, *FOXP3*, *IGF2*, *IREB2*, *MIEF2*, *NOTCH1*, *PDE12*, *SHC1*, and *UCP3*) prognostic model was constructed. Patients in the high-risk group exhibited poorer survival outcomes and a suppressed immune microenvironment compared to the low-risk group. Additionally, except for *IGF2*, abnormal expression levels of hub genes were significantly associated with poor prognosis of BRCA patients. GSVA and GSEA highlighted the involvement of TME-related pathways, such as transforming growth factor beta (TGF-β) and mechanistic target of rapamycin (mTOR) signaling pathways. PPI network identified 4 common genes that interacted with all hub genes. The *in vitro* experiment on the key genes showed a consistent result with the bioinformatics finding.

**Conclusions:** Our study provides insights into the prognostic biomarkers and molecular mechanisms in BRCA, offering potential therapeutic avenues and guiding personalized treatment strategies for improved patient outcomes.

**Keywords:** Breast cancer (BRCA); oxidative phosphorylation (OXPHOS); tumor microenvironment (TME); prognosis; mitochondrion

Submitted Jul 10, 2024. Accepted for publication Nov 13, 2024. Published online Jan 23, 2025.
doi: 10.21037/tcr-24-1181
**View this article at:** https://dx.doi.org/10.21037/tcr-24-1181

## Introduction

Breast cancer (BRCA) is one of the most prevalent malignancies that threaten females' health (1). Approximately 410,000 BRCA new cases occur in China every year, and over 110,000 people die from this disease (2). BRCA is a clinically and molecularly heterogeneous disease (3). In the contemporary landscape of personalized medicine, traditional prognostic markers, including tumor size, histological tumor grade, and lymph node metastasis, have become inadequate for guiding the management of early-diagnosed BRCA patients (4). Recent technological advancements have significantly enhanced our comprehension of the molecular underpinnings of tumor progression and treatment responses (5). Identifying reliable molecular prognostic markers and therapeutic targets remains crucial for refining patient management and improving survival rates.

Among the various biological processes (BP) implicated in cancer biology, oxidative phosphorylation (OXPHOS) has garnered attention due to its role in energy metabolism and its potential implications for tumor therapeutic response (6,7). OXPHOS is a fundamental cellular process that occurs within the mitochondria, involving the production of adenosine triphosphate (ATP) through the transfer of electrons along the mitochondrial respiratory chain (8). Metabolic abnormalities are an important characteristic of cancer, and during the occurrence and development of cancer, many signaling and metabolic pathways change in cancer cells (9). To adapt to the changes, even under aerobic conditions, cancer cells tend to produce ATP through glycolysis (10). However, in recent years, it has been recognized that cancer cells rely on high levels of OXPHOS as an energy source (11). Activation of mitochondrial OXPHOS has also been observed in some cancers, including BRCA (12,13). Regulating OXPHOS signaling pathways could induce BRCA cell cycle arrest and apoptosis, thus inhibiting BRCA proliferation and metastasis (14).

Beyond its direct impact on tumor cells, OXPHOS has also been implicated in shaping the tumor microenvironment (TME), influencing immune cell function, and modulating anti-tumor immune responses (15). The TME comprises a complex network of immune cells, stromal cells, and extracellular matrix components that interact dynamically with cancer cells, influencing tumor progression and treatment sensitivity (16). Understanding the interplay between OXPHOS, the TME, and BRCA biology holds promise for identifying novel prognostic markers and therapeutic targets that may enhance patient outcomes.

This study explored the role of OXPHOS-related genes in BRCA prognosis and their influence on the tumor immune microenvironment. By elucidating the intricate relationship between OXPHOS, tumor biology, and the immune microenvironment, this study aimed to provide insights that may inform the development of personalized therapeutic approaches and improve outcomes for BRCA patients. We present this article in accordance with the TRIPOD reporting checklist (available at https://tcr.amegroups.com/article/view/10.21037/tcr-24-1181/rc).

### Highlight box

**Key findings**

- Nine oxidative phosphorylation (OXPHOS)-related prognostic biomarkers were identified, and a risk model that effectively predicts breast cancer (BRCA) prognosis was constructed.

**What is known and what is new?**

- It is known that mitochondrial genes associated with OXPHOS are upregulated in various cancers, and OXPHOS has been a potential target for BRCA treatment.
- This study developed a nine-gene prognostic model for BRCA based on OXPHOS-related genes and shed light on the intricate interplay between metabolic dysregulation, immune microenvironment, and tumor progression in BRCA.

**What is the implication, and what should change now?**

- These findings provide valuable insights into the molecular mechanisms underlying BRCA progression and may facilitate the development of personalized therapeutic strategies targeting OXPHOS-related pathways and tumor microenvironment components.

## Methods

### *Identification and enrichment analysis of differentially expressed genes (DEGs) in BRCA*

Clinical data and RNA-sequencing data of BRCA were downloaded from The Cancer Genome Atlas (TCGA) database (https://portal.gdc.cancer.gov). After excluding samples with an overall survival (OS) of less than 30 days, 113 normal samples and 1,066 tumor samples were included in the final analysis. The histologic subtype for all tumor samples is presented in the online table (available at https://cdn.amegroups.cn/static/public/tcr-24-1181-1.pdf). DEGs in the normal and tumor samples were identified Using the R package Limma ($P<0.05$ and $|\text{fold change}| \geq 1.5$) and

visualized through a volcano plot. The study was conducted in accordance with the Declaration of Helsinki (as revised in 2013).

Using R packages clusterProfiler and org.Hs.eg.db, Gene Ontology (GO) and Kyoto Encyclopedia of Genes and Genomes (KEGG) enrichment analyses were performed on the DEGs. The GO analysis included BP, cellular component (CC), and molecular function (MF). The criterion was set as $P<0.05$.

### *Screening of differentially expressed OXPHOS-related genes*

The OXPHOS-related genes were screened from the Metabolic Atlas and National Center for Biotechnology Information databases. Using the Venn Diagram package in R, differentially expressed OXPHOS-related genes were then screened out by intersecting the DEGs and OXPHOS-related genes.

### *Identification of hub prognostic features and construction of risk model*

To identify genes related to the prognosis of BRCA patients, univariate Cox regression analysis was performed on the differentially expressed OXPHOS-related genes. After reducing redundancy in the predictive framework through the least absolute shrinkage and selection operator (LASSO) regression, hub prognostic genes were identified using multivariate Cox regression. The LASSO regression was conducted using the R package glmnet. The hub prognostic genes were then applied to construct a prognostic model for BRCA patients. The risk scores for each TCGA-BRCA patient were calculated as: risk score = $exp_{RNA1}*coef_{RNA1}$ + $exp_{RNA2}*coef_{RNA2}$ + … + $exp_{RNAi}*coef_{RNAi.}$

The TCGA-BRCA patients were divided into low- and high-risk groups based on the optimal truncation value of risk scores. The differences in OS in the low- and high-risk groups were shown using Kaplan-Meier (K-M) curves. Time-dependent receiver operating characteristic (ROC) curves at 3-, 5-, and 10-year were constructed using the R package survival. The area under the curve (AUC) value was calculated to reflect the prognostic performance of the model.

### *Gene set variation analysis (GSVA) and gene set enrichment analysis (GSEA)*

Biological enrichment differences in the low- and high-risk groups were determined using the GSVA analysis. GSVA analysis was performed through R packages GSEABase and GSVA. h.all.v2023.2.Hs.symbols was set as a reference gene set, and the results were visualized using ggplot2. GSEA analysis was conducted to screen hub gene-related pathways using the GSVA package.

### *TME analysis*

Immune cell infiltration between the low- and high-risk groups was detected through the CIBERSORT algorithm of the IBOR package in R. Immune checkpoint-related genes were obtained from a literature (17). Expression levels of these genes in the low- and high-risk groups were further explored. Tumor immune dysfunction and exclusion (TIDE) score was measured on the TIDE website (http://tide.dfci.harvard.edu/).

### *Construction of protein-protein interaction (PPI) network*

Gene sets interacting with hub genes were identified from the genetic perturbation similarity analysis (GPSA) database (https://www.gpsadb.com/). A Venn diagram was utilized to acquire the common genes that modulate all of the hub genes. The interactions among hub genes and their interactions with the common genes were visualized through the PPI networks. The PPI networks were generated by the Search Tool for the Retrieval of Interacting Genes/Proteins (STRING) database (http://stringdb.org) and visualized using Cytohubba in Cytoscape 3.7.0.

### *Drug sensitivity analysis*

Drug sensitivity analysis of hub genes was conducted using Gene Set Cancer Analysis (GSCA) (https://guolab.wchscu.cn/GSCA/#/). The correlation between hub genes and the sensitivity of potential drugs was assessed using the Pearson method.

### *Cell culture*

Wuhan Pricella Biotechnology Co., Ltd. provided MCF-12A (CL-0791) human mammary epithelial cell line and MDA-MB-231 (CL-0150) human BRCA cell line. Both cell lines were maintained in Dulbecco's Modified Eagle's Medium (Gibco, NY, USA) with 10% fetal bovine serum

**Table 1** Primer sequences used in this study

| Gene | Sequences |
|---|---|
| *FOXP3*-forward | 5'-GTGGCCCGGATGTGAGAAG-3' |
| *FOXP3*-reverse | 5'-GGAGCCCTTGTCGGATGATG-3' |
| *SHC1*-forward | 5'-TACTTGGTTCGGTACATGGGT-3' |
| *SHC1*-reverse | 5'-CTGAGTCCGGGTGTTGAAGTC-3' |
| *NOTCH1*-forward | 5'-GAGGCGTGGCAGACTATGC-3' |
| *NOTCH1*-reverse | 5'-CTTGTACTCCGTCAGCGTGA-3' |
| *IGF2*-forward | 5'-GTGGCATCGTTGAGGAGTG-3' |
| *IGF2*-reverse | 5'-CACGTCCCTCTCGGACTTG-3' |
| *UCP3*-forward | 5'-TGTTTTGCTGACCTCGTTACC-3' |
| *UCP3*-reverse | 5'-GACGGAGTCATAGAGGCCGAT-3' |
| *GAPDH*-forward | 5'-GGAGCGAGATCCCTCCAAAAT-3' |
| *GAPDH*-reverse | 5'-GGCTGTTGTCATACTTCTCATGG-3' |

GAPDH, glyceraldehyde 3-phosphate dehydrogenase.

under standard conditions of 37 ℃ and 5% $CO_2$.

### *Quantitative real-time polymerase chain reaction (qRT-PCR)*

TRIzol reagent (Invitrogen, CA, USA) was employed to isolate total RNA following the manufacturer's instructions. The reverse transcription of total RNA to complementary DNA was conducted using the PrimeScript RT reagent kit (Takara, Dalian, China). Subsequently, qRT-PCR was carried out utilizing the Hieff UNICON Universal Blue qPCR SYBR Green Master Mix (Yeasen, Shanghai, China) on an ABI7900HT System. The relative messenger RNA (mRNA) expression levels were calculated using the $2^{-\Delta\Delta Ct}$ method, and glyceraldehyde 3-phosphate dehydrogenase (GAPDH) was set as the internal control. The primer sequences used in this study are shown in *Table 1*.

### *Statistical analysis*

All statistical analyses were performed using R software version 4.2.0, SPSS, and GraphPad Prism 8.0.2. The predictive performance of hub genes was evaluated using the K-M curve. Student's *t*-test was used to compare the differences between the two groups, and the Pearson method was used for correlation analysis. Statistical significance was set as $P<0.05$.

## Results

### *Identification of differentially expressed OXPHOS-related genes in BRCA*

In total, 9,390 DEGs were identified from the TCGA dataset, with 3,672 down-regulated genes and 5,718 up-regulated genes in the tumor samples. The results were visualized in a volcano plot (*Figure 1A*). Furthermore, biological function of these DEGs was explored. The top five BP terms were cellular protein metabolic process, macromolecule biosynthetic process, establishment of localization, transport, and system development (*Figure 1B*). CCs of these DEGs were major related to cytosol, nuclear part, protein-containing complex, endomembrane system, and non-membrane-bounded organelle (*Figure 1C*). The MFs were mainly associated with catalytic activity, cation binding, metal ion binding, nucleic acid binding, and anion binding (*Figure 1D*). KEGG pathways were mainly enriched in the phosphatidylinositol 3-kinase (PI3K)-protein kinase B (Akt) signaling pathway, mitogen-activated protein kinases (MAPK) signaling pathway, focal adhesion, Ras-associated protein 1 (Rap1) signaling pathway, and cellular senescence (*Figure 1E*).

In addition, after intersecting the DEGs and OXPHOS-related genes, 234 differentially expressed OXPHOS-related genes were obtained (*Figure 1F*). These overlapping genes were used for further analysis.

### *Identification and evaluation of prognostic features in OXPHOS-related genes*

Subsequently, univariate Cox regression analysis was performed on the 234 differentially expressed OXPHOS-related genes and 27 genes with statistical significance were identified (*Figure 2A*). The LASSO regression analysis further screened out 22 genes related to prognosis with the optimal λ value of 0.0046 (*Figure 2B*). Finally, the multivariate Cox regression analysis filtered nine hub genes including *ATP5PF*, *FOXP3*, *IGF2*, *IREB2*, *MIEF2*, *NOTCH1*, *PDE12*, *SHC1*, and *UCP3* (*Figure 2C*). A BRCA prognostic model was then constructed based on the nine hub genes. The risk score of each sample in the TCGA dataset was calculated as follows: risk score =0.018**ATP5PF* – 0.17**FOXP3* + 0.024**IGF2* + 0.06**IREB2* – 0.088**MIEF2* + 0.035**NOTCH1* – 0.152**PDE12* + 0.021**SHC1* –

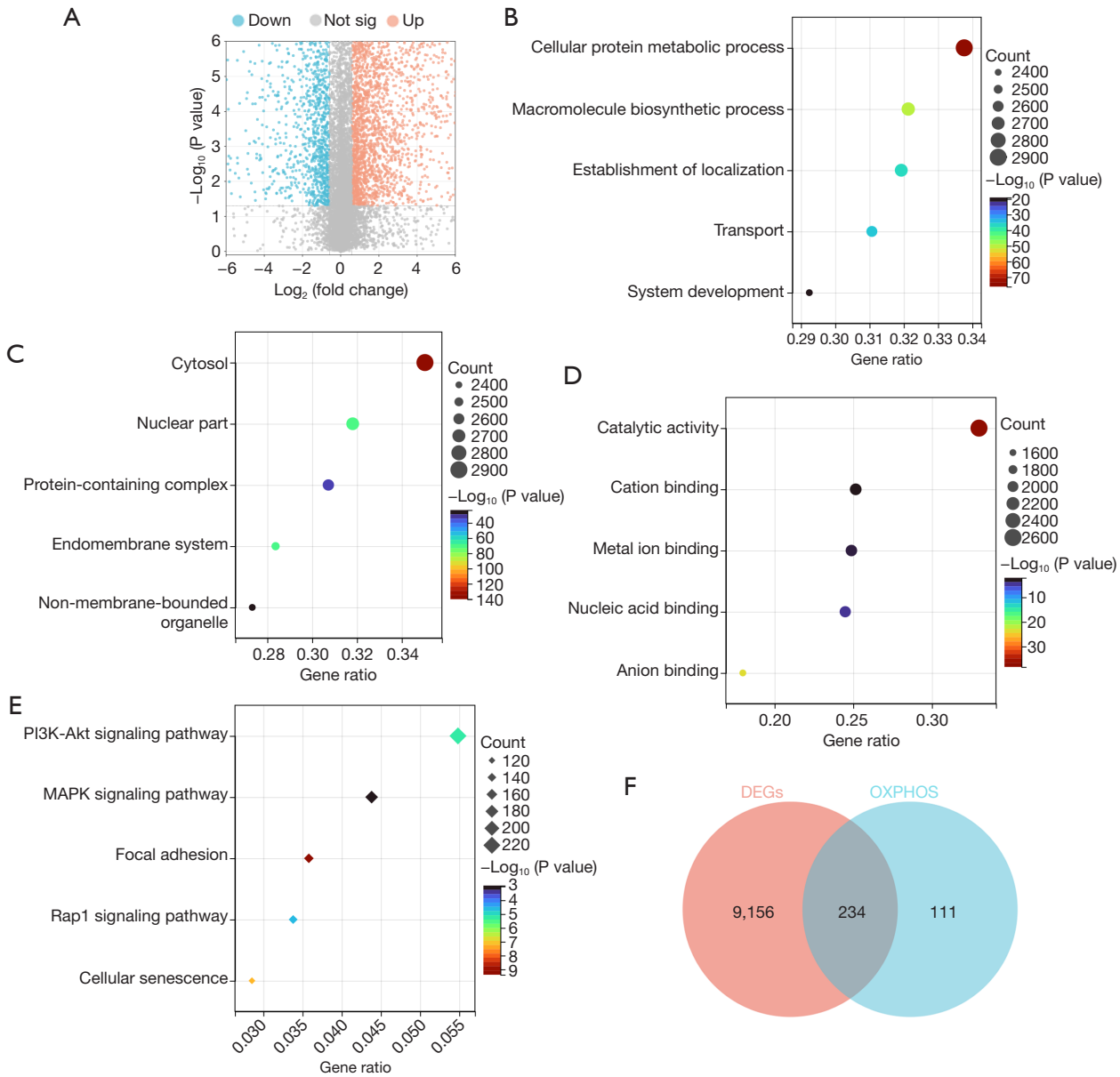


**Figure 1** Identification of differentially expressed OXPHOS-related genes in BRCA. (A) Volcano plot showed the DEGs between the normal and tumor samples in the TCGA-BRCA cohort. (B-D) GO terms related to DEGs, including BP (B), CC (C), and MF (D). (E) KEGG pathways associated with DEGs. (F) Venn diagram revealed the overlapping genes between DEGs and OXPHOS-related genes. Sig, significant; OXPHOS, oxidative phosphorylation; BRCA, breast cancer; DEGs, differentially expressed genes; TCGA, The Cancer Genome Atlas; GO, Gene Ontology; BP, biological process; CC, cellular component; MF, molecular function; KEGG, Kyoto Encyclopedia of Genes and Genomes; PI3K, phosphatidylinositol 3-kinase; Akt, protein kinase B; MAPK, mitogen-activated protein kinases; Rap1, Ras-associated protein 1.

0.757**UCP3*.

Based on the optimal truncation value of the risk scores, patients in the TCGA-BRCA dataset were categorized into low- and high-risk groups. The K-M curve showed that individuals in the low-risk group had a higher survival probability than those in the high-risk group (*Figure 3A*). The AUCs of the time-dependent ROC curve at 3-, 5-, and 10-year were 0.68, 0.69, and 0.75, respectively (*Figure 3B*). Subsequently, K-M survival was conducted to assess the model's performance across different BRCA subtypes. As

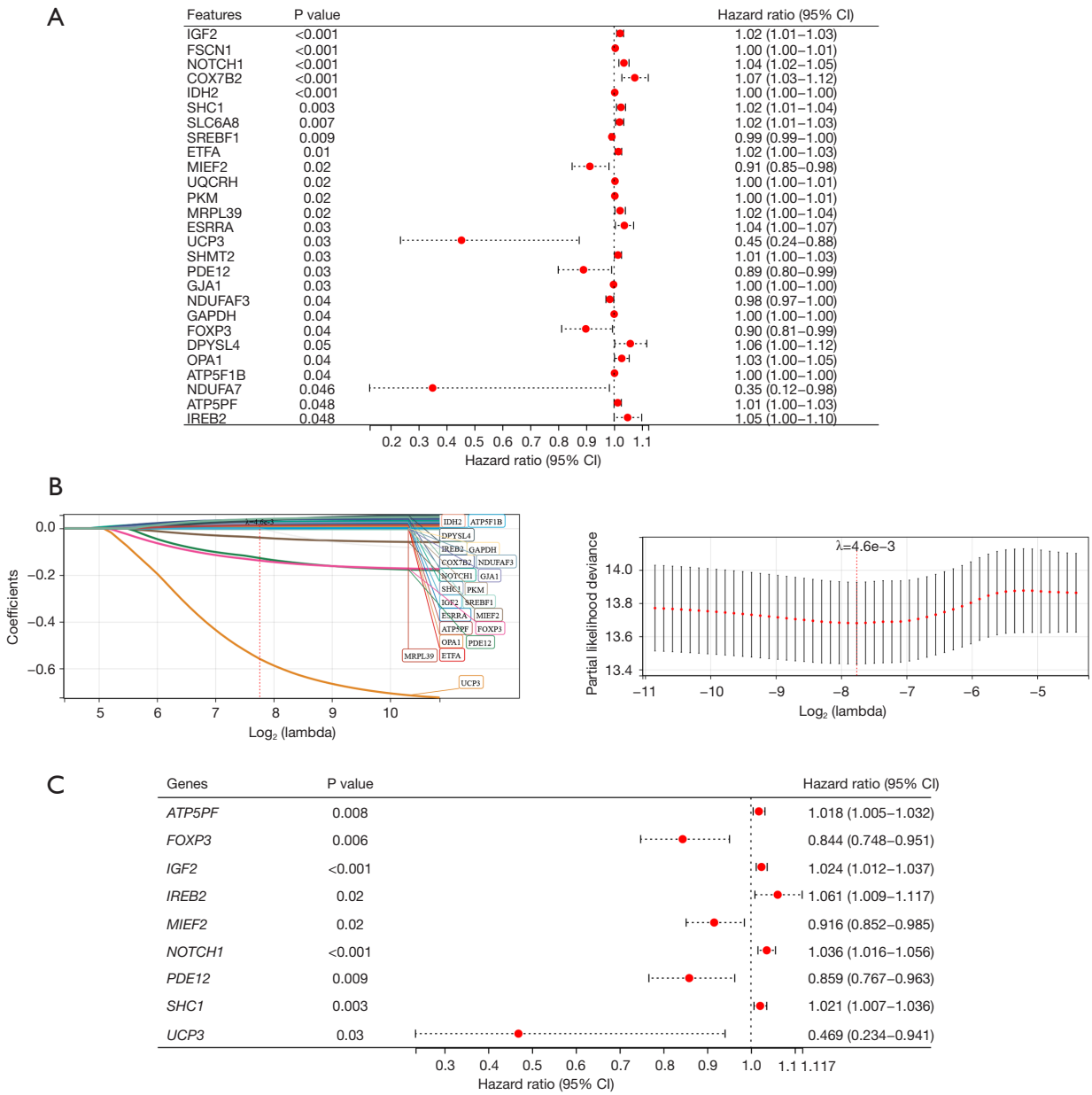


**Figure 2** Identification of hub genes related to prognosis. (A) Univariate Cox regression analysis was performed on 234 differentially expressed OXPHOS-related genes. (B) Correlation coefficient change curve and cross-validation curve in the LASSO regression analysis. (C) Nine hub genes were identified using multivariate Cox regression analysis; Hazard ratio >1 represents risk factor, and hazard ratio <1 represents protective factor. OXPHOS, oxidative phosphorylation; LASSO, least absolute shrinkage and selection operator; CI, confidence interval.

illustrated in Figure S1, the high-risk group consistently exhibited poorer prognoses compared to the low-risk group in BRCA patients with human epidermal growth factor receptor 2-positive (HER2$^+$), triple-negative breast cancer (TNBC), luminal A, and luminal B subtypes. These results revealed that the nine-gene prognostic risk model performed well in predicting the survival of BRCA patients.

### *GSVA and GSEA analyses*

To further elucidate the pathways related to the prognostic risk model, GSVA analysis was performed between the

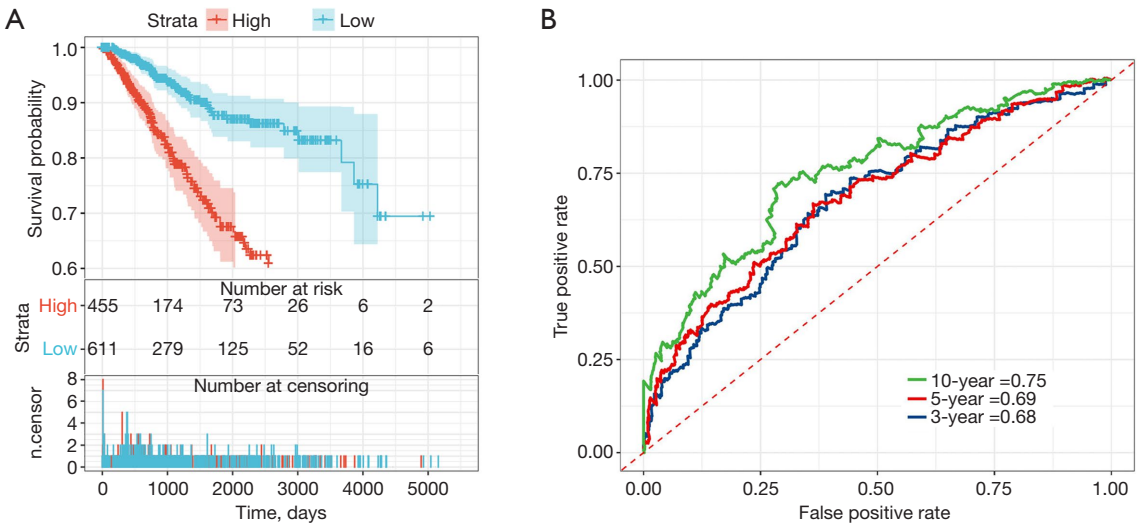


**Figure 3** Evaluation of the prognostic risk model. (A) Kaplan-Meier curve for overall survival of patients in the low- and high-risk groups based on the TCGA-BRCA cohort. (B) Time-dependent receiver operating characteristic curves at 3-, 5-, and 10-year. TCGA, The Cancer Genome Atlas; BRCA, breast cancer.

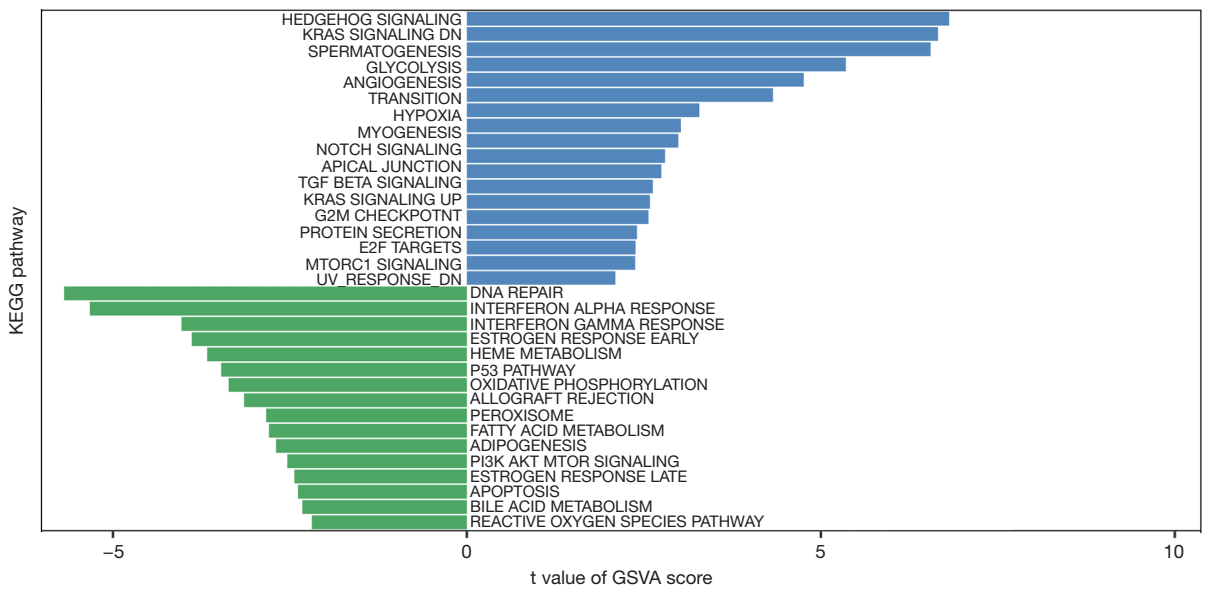


**Figure 4** Risk model-related gene set variation analysis. Blue means activated, and green means suppressed. KEGG, Kyoto Encyclopedia of Genes and Genomes; GSVA, gene set variate analysis.

low- and high-risk groups. The NOTCH signaling, transforming growth factor beta (TGF-β) signaling, and mechanistic target of rapamycin complex 1 (mTORC1) signaling were activated, while the p53 pathway and PI3K-Akt-mTOR signaling were suppressed (*Figure 4*).

Additionally, GSEA analysis was performed to elucidate the hub gene-related pathways. As shown in *Figure 5*, these hub genes were mainly involved in TGF-β, mechanistic target of rapamycin (mTOR), and Wnt signaling pathways. Combined with GSVA and GSEA analysis, the results showed that the risk model as well as the individual gene in the model had an intimated relation with TME.

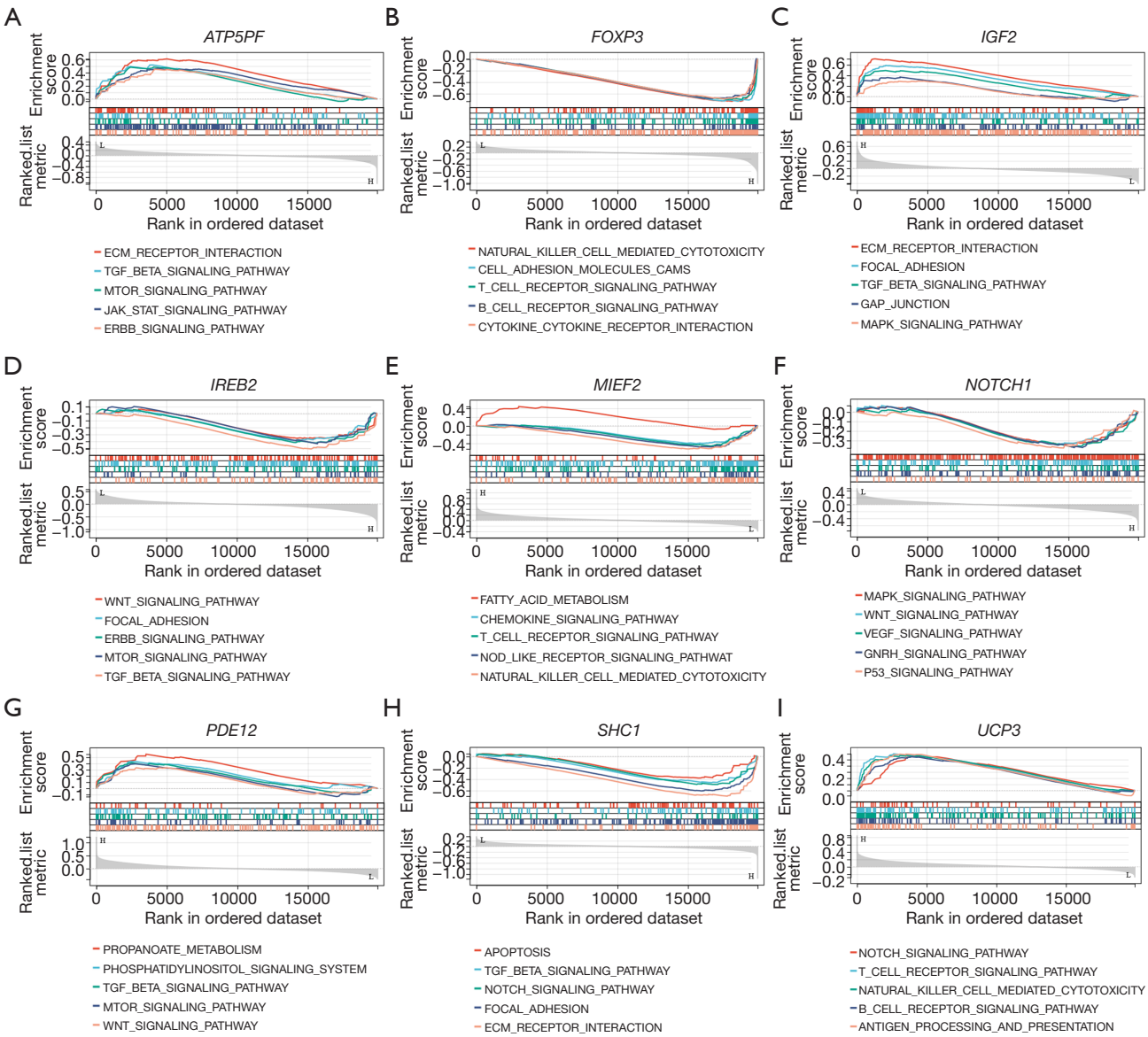


**Figure 5** GSEA analysis of 9 hub genes. (A-I) GSEA analysis for *ATP5PF* (A), *FOXP3* (B), *IGF2* (C), *IREB2* (D), *MIEF2* (E), *NOTCH1* (F), *PDE12* (G), *SHC1* (H), and *UCP3* (I). L means a low expression of the gene, and H means a high expression of the gene. GSEA, gene set enrichment analysis; ECM, extracellular matrix; MAPK, mitogen-activated protein kinases; mTOR, mechanistic target of rapamycin.

### *Risk model-related TME analysis*

We have demonstrated the tight association of the risk model with TME. Besides, various immune cells as important components in TME play essential roles in cancer pathogenesis (18). These triggered us to explore the TME between two risk groups. We compared the differences in immune cell infiltration between low- and high-risk groups. The number of natural killer (NK) cells resting (P<0.001), macrophages M0 (P<0.001), macrophages M2 (P=0.001), and dendritic cells activated (P=0.02) was significantly richer in the high-risk group (*Figure 6A*). Cell abundance of T cells CD8 (P<0.001), T cells CD4 memory resting (P=0.03), T cells CD4 memory activated (P=0.02), T cells follicular helper (P=0.005), T cells regulatory (Tregs) (P=0.03), NK cells activated (P=0.006), monocytes (P=0.008), macrophage M1 (P=0.02), dendritic cells resting (P=0.003), and mast cells resting (P<0.001) was significantly

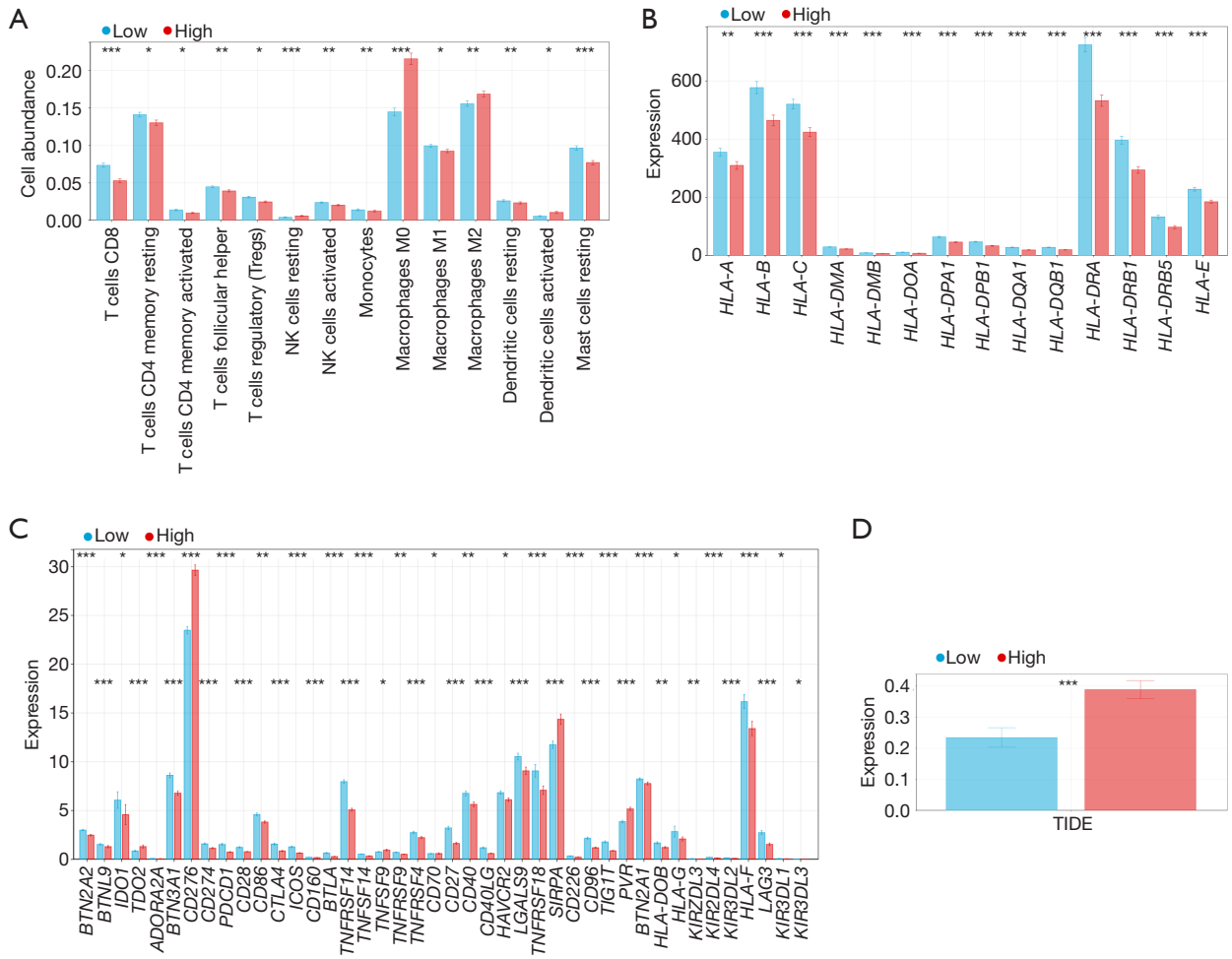


**Figure 6** Risk model-related TME analysis. (A) Immune cell infiltration in the low- and high-risk groups. (B,C) Expression levels of immune checkpoint-related genes in the low- and high-risk groups. (D) TIDE scores in the low- and high-risk groups. *, P<0.05; **, P<0.01; ***, P<0.001. TME, tumor microenvironment; TIDE, tumor immune dysfunction and exclusion; NK, natural killer.

higher in the low-risk group (*Figure 6A*). Furthermore, we explored the expression of immune checkpoint-related genes in the low- and high-risk groups. Except for *TDO2*, *CD276*, *TNFSF9*, *SIRPA*, and *PVR*, most of the immune checkpoint-related genes were significantly downregulated in the high-risk group, especially *HLA* (*Figure 6B*,*6C*). There was a higher TIDE score in the high-risk group than in the low-risk group, with statistical significance (P<0.001, *Figure 6D*). The above findings indicated that a high-risk score was associated with a suppressive immune microenvironment.

### *Expression and survival analyses of nine hub genes*

Expression levels of the identified 9 hub genes and their association with the OS of BRCA patients were analyzed to investigate the role of these genes in the prognosis of BRCA. In comparison with the low-risk group, expression levels of *ATP5PF*, *IREB2*, *NOTCH1*, and *SHC1* were significantly elevated while expression of *FOXP3*, *MIEF2*, *PDE12*, and *UCP3* was reduced in the high-risk group (all P<0.001, *Figure 7A*). BRCA patients with higher levels of *ATP5PF* (P=0.02), *IREB2* (P=0.03), *NOTCH1* (P=0.04), and *UCP3* (P=0.02) as well as lower levels of *FOXP3* (P=0.003), *MIEF2* (P=0.03), *PDE12* (P=0.01), and *SHC1* (P=0.01) had a poor prognosis (*Figure 7B-7J*).

### *PPI network construction*

Furthermore, the gene sets that affect the expression of

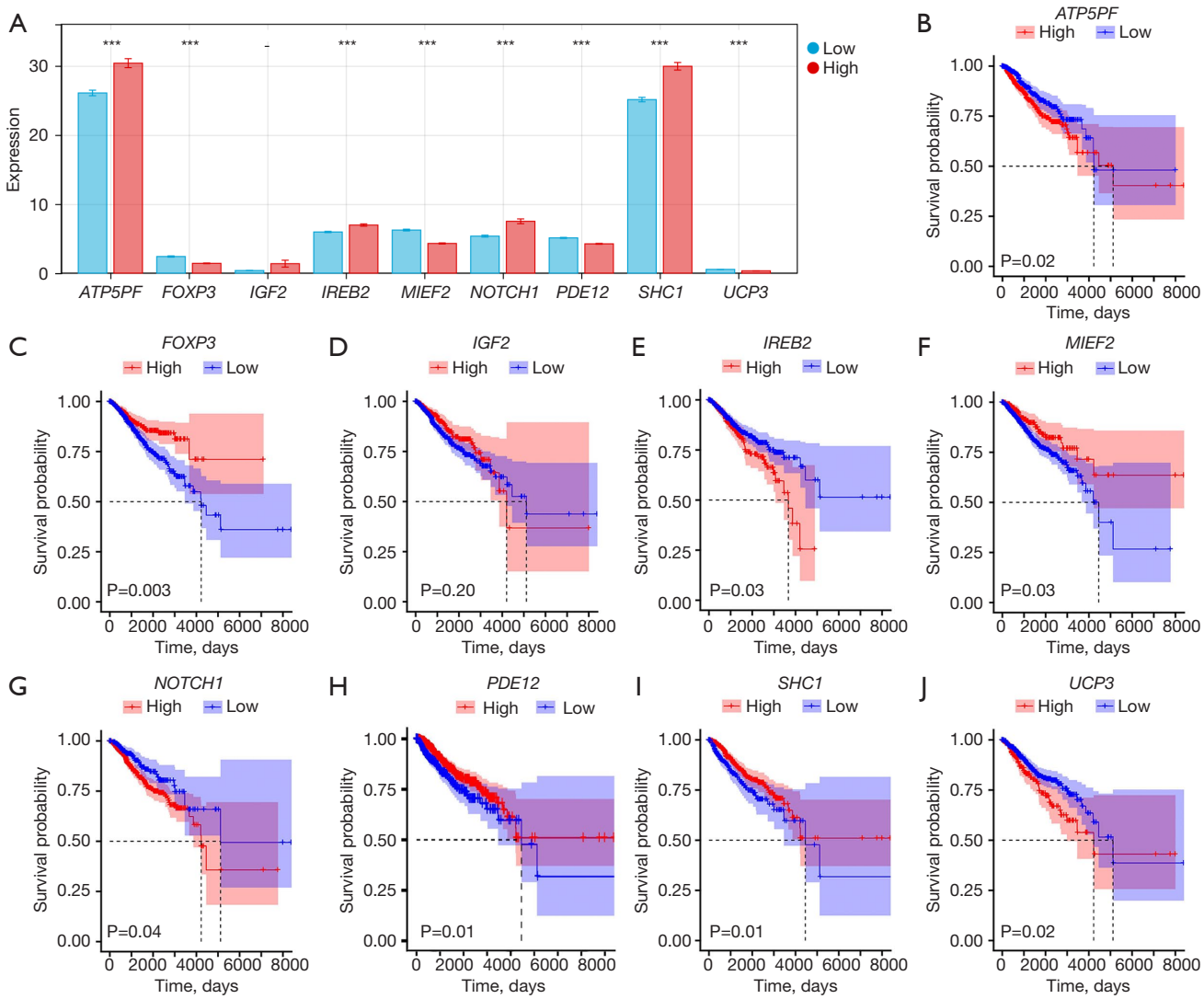


**Figure 7** Expression levels and survival analysis of the hub genes. (A) Expression levels of 9 hub genes in the low- and high-risk groups. ***, P<0.001; "-" means no significance. (B-J) Kaplan-Meier curves for overall survival between groups differentiated by high-expression or low-expression of 9 hub genes.

these 9 hub genes were then screened out from the GPSA website, and four common genes (*TCF3*, *UPF1*, *LOXL2*, and *PRPF8*) interacted with the expression of all 9 hub genes were obtained (*Figure 8A*). The interactions among 9 hub genes and their interactions with the 4 overlapping genes were visualized in *Figure 8B,8C*. It revealed that *FOXP3*, *IGF2*, *SHC1*, *NOTCH1*, and *UCP3* were interacted with each other (*Figure 8A*).

### *In vitro validation of hub gene expression*

qRT-PCR was further performed on the genes that interacted with each other in the PPI network to validate their expression in cells. *FOXP3* expression was reduced while the other four genes' expression (*NOTCH1*, *IGF2*, *SHC1*, and *UCP3*) was elevated in the MDA-MB-231 cells compared with the MCF-12A cells (P<0.001, *Figure 9*).

### *Drug sensitivity analysis*

Moreover, 30 potential drugs for BRCA were searched from the Genomics of Drug Sensitivity in Cancer (GDSC) database. The correlation of 9 hub gene expression levels with the sensitivity of 30 potential drugs is shown in *Figure 10*.

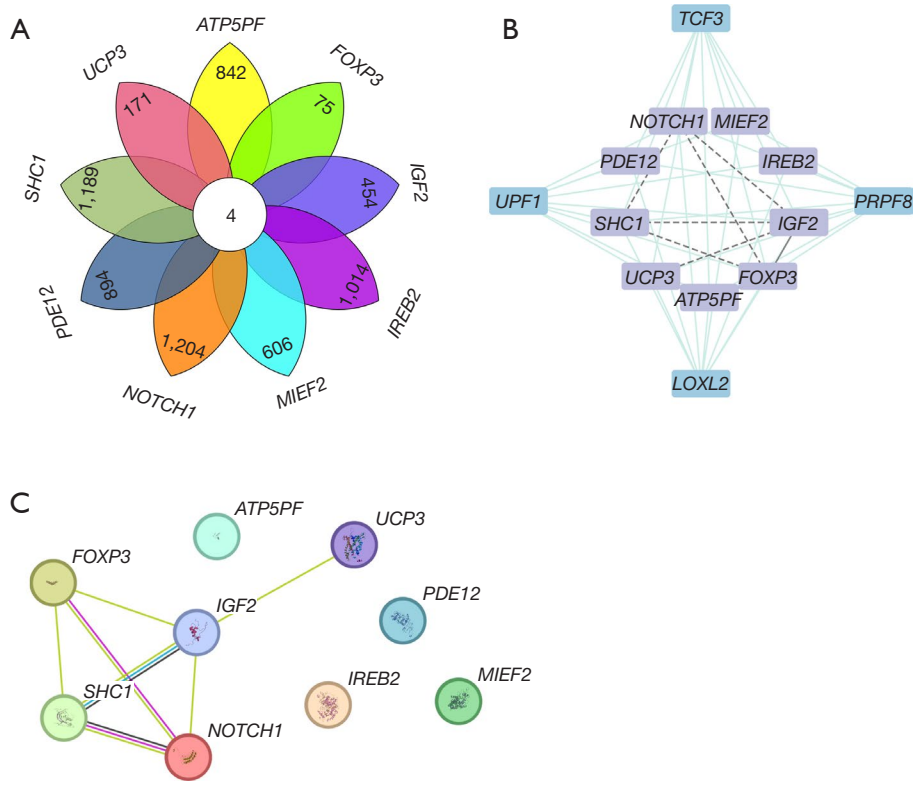


**Figure 8** PPI network construction. (A) Four gene sets that affect the expression of 9 hub genes were identified. (B) PPI network of 9 hub genes with the four common interacting genes. (C) PPI network of the 9 hub genes. PPI, protein-protein interaction.

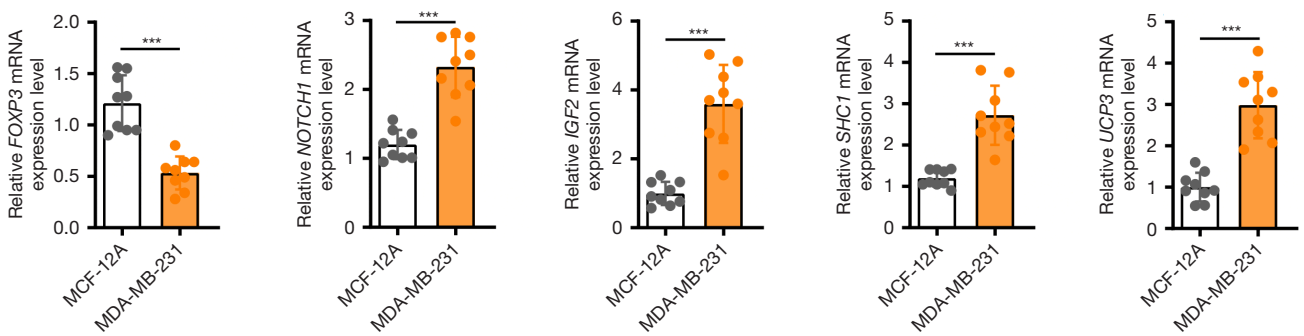


**Figure 9** *In vitro* validation of hub gene expression. ***, P<0.001.

Expression of *MIEF2*, *SHC1*, and *IGF2* was mainly positively related to these 30 drugs, while the other 6 gene expression levels were negatively associated with most of these 30 drugs.

## Discussion

In recent years, more and more evidence has shown that mitochondrial genes associated with OXPHOS are upregulated in various cancers (19). OXPHOS has been a potential target for BRCA treatment. A recent study revealed a drug 9S1R-NulloPT that could kill TNBC cells by targeting mitochondrial metabolic pathways (20). El-Botty *et al.* demonstrated that treatment with the OXPHOS inhibitor IACS-010759 significantly inhibits tumor growth, particularly in endocrine and palbociclib-resistant metastatic estrogen receptor-positive (ER$^+$) BRCA (21). However,

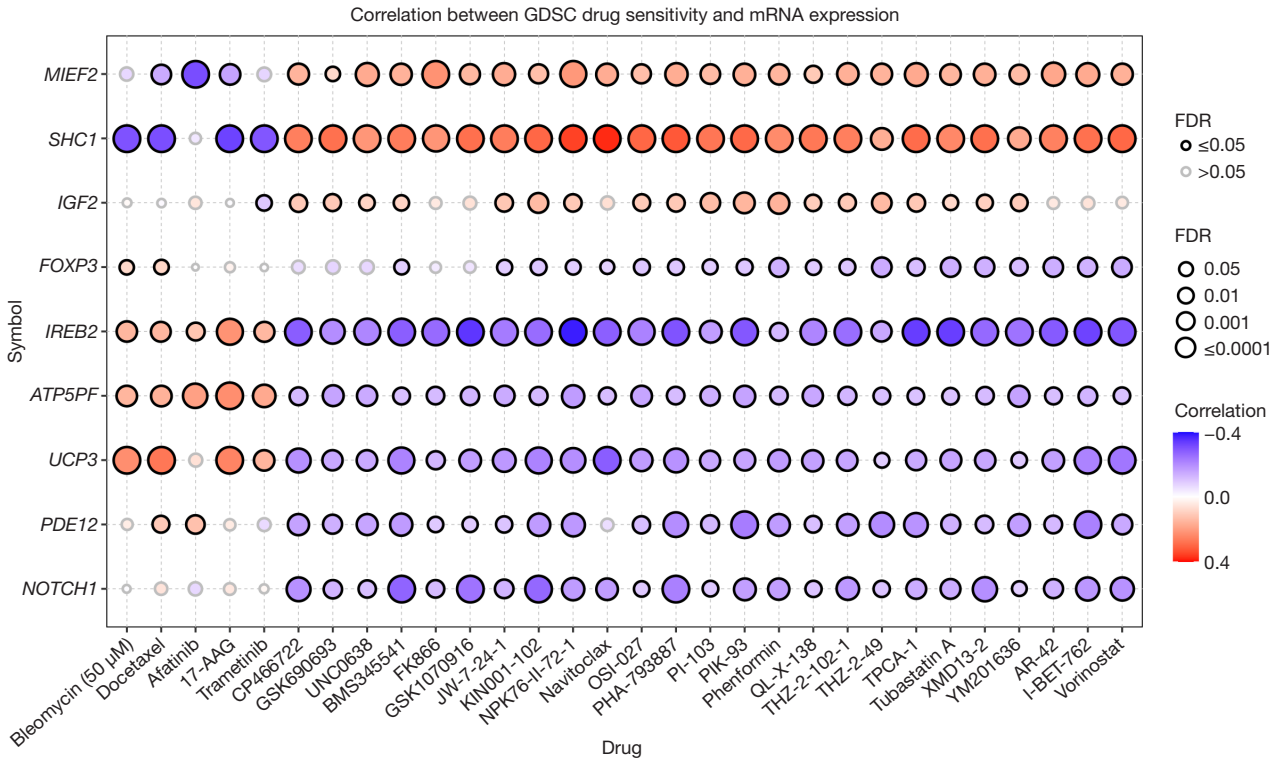


**Figure 10** Correlation between drug sensitivity and mRNA expression of 9 hub genes. GDSC, Genomics of Drug Sensitivity in Cancer; FDR, false discovery rate; mRNA, messenger RNA.

few studies have systematically screened OXPHOS genes associated with BRCA prognosis. This study attempted to screen potential prognostic biomarkers and explore their potential roles in regulating the immune microenvironment, thereby providing evidence for identifying new therapeutic targets and pathways for BRCA.

Functional enrichment analysis indicates that DEGs in BRCA were associated with biological functions such as cellular protein metabolism process, macromolecular biosynthesis process, and transport. We particularly focused on the macromolecular biosynthesis process (namely synthetic metabolism). Active metabolism is crucial for tumor growth, and a common feature of cancer cells is their ability to undergo metabolic reprogramming to sustain macromolecular production (22). OXPHOS pathways provide the biological energy demands and lead to macromolecular synthesis to promote cancer cell proliferation (8). Metastatic BRCA heavily relies on OXPHOS (21). Based on TCGA data and LASSO Cox regression analysis, we identified 9 OXPHOS-related prognosis biomarkers, including *ATP5PF*, *FOXP3*, *IGF2*, *IREB2*, *MIEF2*, *NOTCH1*, *PDE12*, *SHC1*, and *UCP3*. The nine identified hub genes are integral to the OXPHOS pathway, influencing mitochondrial function and energy production in BRCA. As a component of ATP synthase, *ATP5PF* enhances ATP production (23). *FOXP3*, known for its role in regulatory T cells, also has been reported to drive OXPHOS (24). *IGF2*, a growth factor associated with cellular proliferation, exerts its effects by preprogramming maturing macrophages to commit OXPHOS (25). *IREB2*, involved in iron metabolism, affects mitochondrial function because iron is essential for OXPHOS (26). *MIEF2* impacts mitochondrial dynamics, which can influence the efficiency of OXPHOS (27). *NOTCH1*, known for modulating cellular signaling, has been associated with mitochondrial metabolism and affects OXPHOS pathways (28). *PDE12*, which is involved in cyclic nucleotide metabolism, may influence signaling pathways that intersect with OXPHOS regulation (29). *SHC1* participates in signaling pathways that impact metabolism and could activate OXPHOS (30). *UCP3*, which regulates mitochondrial uncoupling, affects both energy expenditure and OXPHOS efficiency (31). In our study, the risk model established based on these nine hub OXPHOS-related genes effectively predicted the 3-, 5-,

and 10-year survival rates of BRCA patients.

Further analysis provided insights into the molecular mechanisms underlying the roles of the nine hub genes in BRCA. The hub genes were found to be associated with key signaling pathways involved in TME regulation, such as TGF-β, mTOR, and Wnt signaling. Dysregulated TGF-β signaling within the TME promotes immunosuppression, angiogenesis, and metastasis in BRCA (32). Similarly, aberrant mTOR signaling contributes to tumor cell survival, proliferation, and immune evasion, while dysregulated Wnt signaling promotes cancer stemness, epithelial-to-mesenchymal transition, and immune evasion (33). These pathways collectively influence TME dynamics by modulating immune cell recruitment, angiogenesis, and cytokine secretion, thereby impacting disease progression and therapeutic responses (34). The hub genes we identified may alter the TME and affect the development of BRCA by potentially influencing these pathways.

The metabolic changes in cancer cells are closely associated with the abnormal functions of immune cells and immune factors, leading to tumor immune escape (35). The intricate crosstalk between immune cells and cancer cells is a key mechanism in regulating cancer progression (36). Metabolic dysregulation in BRCA leads to restricted energy generation in the TME, ultimately resulting in impaired cellular function (37). Therefore, we analyzed the immune microenvironment and found that the activation levels of CD8 T cells, CD4 memory T cells, NK cells, and M1 macrophages were higher in the low-risk group, while M2 macrophages and dendritic cells were enriched in the high-risk group. CD8 T cells possess immunosuppressive functions (38). T memory cells express high levels of immune checkpoint molecules, contributing to suppressing tumors, and have been shown to actively participate in immune surveillance of BRCA (39). Immune checkpoint-related gene *HLA* was observed to be upregulated in the low-risk group. *HLA* is an important mediator of anti-tumor immune responses (40). We speculate that high levels of CD8 T cells and CD4 memory T cells were associated with the high expression of *HLA* in the low-risk group. M1 macrophages trigger anti-tumor immune signaling and are associated with tumor-killing capabilities. Conversely, M2 macrophages exert pro-tumor effects, associated with angiogenesis, metastasis, and adaptive immune suppression (41). Correspondingly, we observed elevated CD40 expression in the low-risk group, a typical biomarker of M1 macrophages. Additionally, NK cells participate in anti-tumor immune responses by producing pro-inflammatory cytokines or directly killing tumor cells, playing a positive role in cancer immune surveillance (42,43). All in all, our result revealed an inhibited immune microenvironment in the high-risk group, thus more likely to suffer from BRCA.

## Conclusions

In conclusion, we identified nine OXPHOS-related prognosis biomarkers and developed a risk model for predicting BRCA prognosis, which effectively predicts survival rates at various time points. Furthermore, our findings shed light on the intricate interplay between metabolic dysregulation, immune microenvironment, and tumor progression in BRCA. Our study elucidated the molecular mechanisms underlying the roles of the identified hub genes in BRCA, highlighting their associations with key signaling pathways involved in TME regulation, such as TGF-β, mTOR, and Wnt signaling. These findings provide valuable insights into the molecular mechanisms underlying BRCA progression and may facilitate the development of personalized therapeutic strategies targeting OXPHOS-related pathways and TME components.

## Acknowledgments

None.

## Footnote

*Reporting Checklist:* The authors have completed the TRIPOD reporting checklist. Available at https://tcr.amegroups.com/article/view/10.21037/tcr-24-1181/rc

*Data Sharing Statement:* Available at https://tcr.amegroups.com/article/view/10.21037/tcr-24-1181/dss

*Peer Review File:* Available at https://tcr.amegroups.com/article/view/10.21037/tcr-24-1181/prf

*Funding:* None.

*Conflicts of Interest:* All authors have completed the ICMJE uniform disclosure form (available at https://tcr.amegroups.com/article/view/10.21037/tcr-24-1181/coif). The authors have no conflicts of interest to declare.

*Ethical Statement:* The authors are accountable for all aspects of the work in ensuring that questions related

to the accuracy or integrity of any part of the work are appropriately investigated and resolved. The study was conducted in accordance with the Declaration of Helsinki (as revised in 2013).



## References

1. Liang J, Ye C, Chen K, et al. Non-coding RNAs in breast cancer: with a focus on glucose metabolism reprogramming. Discov Oncol 2023;14:72.
2. Wu H, Jiao Y, Guo X, et al. METTL14/miR-29c-3p axis drives aerobic glycolysis to promote triple-negative breast cancer progression though TRIM9-mediated PKM2 ubiquitination. J Cell Mol Med 2024;28:e18112.
3. Neves Rebello Alves L, Dummer Meira D, Poppe Merigueti L, et al. Biomarkers in Breast Cancer: An Old Story with a New End. Genes (Basel) 2023;14:1364.
4. Barzaman K, Karami J, Zarei Z, et al. Breast cancer: Biology, biomarkers, and treatments. Int Immunopharmacol 2020;84:106535.
5. Mehta S, Shelling A, Muthukaruppan A, et al. Predictive and prognostic molecular markers for cancer medicine. Ther Adv Med Oncol 2010;2:125-48.
6. Ashton TM, McKenna WG, Kunz-Schughart LA, et al. Oxidative Phosphorylation as an Emerging Target in Cancer Therapy. Clin Cancer Res 2018;24:2482-90.
7. Liu Y, Sun Y, Guo Y, et al. An Overview: The Diversified Role of Mitochondria in Cancer Metabolism. Int J Biol Sci 2023;19:897-915.
8. Greene J, Segaran A, Lord S. Targeting OXPHOS and the electron transport chain in cancer; Molecular and therapeutic implications. Semin Cancer Biol 2022;86:851-9.
9. Yoshida GJ. Metabolic reprogramming: the emerging concept and associated therapeutic strategies. J Exp Clin Cancer Res 2015;34:111.
10. Bai R, Meng Y, Cui J. Therapeutic strategies targeting metabolic characteristics of cancer cells. Crit Rev Oncol Hematol 2023;187:104037.
11. Yang Y, An Y, Ren M, et al. The mechanisms of action of mitochondrial targeting agents in cancer: inhibiting oxidative phosphorylation and inducing apoptosis. Front Pharmacol 2023;14:1243613.
12. Wu Y, Zhang X, Wang Z, et al. Targeting oxidative phosphorylation as an approach for the treatment of ovarian cancer. Front Oncol 2022;12:971479.
13. Ghosh P, Vidal C, Dey S, et al. Mitochondria Targeting as an Effective Strategy for Cancer Therapy. Int J Mol Sci 2020;21:3363.
14. Li J, Liu X, Chen L, et al. Isopimaric acid, an ion channel regulator, regulates calcium and oxidative phosphorylation pathways to inhibit breast cancer proliferation and metastasis. Toxicol Appl Pharmacol 2023;462:116415.
15. Qiu X, Li Y, Zhang Z. Crosstalk between oxidative phosphorylation and immune escape in cancer: a new concept of therapeutic targets selection. Cell Oncol (Dordr) 2023;46:847-65.
16. Li Z, Sun C, Qin Z. Metabolic reprogramming of cancer-associated fibroblasts and its effect on cancer cell reprogramming. Theranostics 2021;11:8322-36.
17. Hu FF, Liu CJ, Liu LL, et al. Expression profile of immune checkpoint genes and their roles in predicting immunotherapy response. Brief Bioinform 2021;22:bbaa176.
18. de Visser KE, Joyce JA. The evolving tumor microenvironment: From cancer initiation to metastatic outgrowth. Cancer Cell 2023;41:374-403.
19. Uslu C, Kapan E, Lyakhovich A. Cancer resistance and metastasis are maintained through oxidative phosphorylation. Cancer Lett 2024;587:216705.
20. Ali N, Wolf C, Kanchan S, et al. 9S1R nullomer peptide induces mitochondrial pathology, metabolic suppression, and enhanced immune cell infiltration, in triple-negative breast cancer mouse model. Biomed Pharmacother 2024;170:115997.
21. El-Botty R, Morriset L, Montaudon E, et al. Oxidative phosphorylation is a metabolic vulnerability of endocrine therapy and palbociclib resistant metastatic breast cancers. Nat Commun 2023;14:4221.
22. Koundouros N, Poulogiannis G. Reprogramming of fatty acid metabolism in cancer. Br J Cancer 2020;122:4-22.
23. Zhuang Y, Chai J, Abdelsattar MM, et al. Transcriptomic and metabolomic insights into the roles of exogenous β-hydroxybutyrate acid for the development of rumen epithelium in young goats. Anim Nutr 2023;15:10-21.
24. Howie D, Cobbold SP, Adams E, et al. Foxp3 drives

oxidative phosphorylation and protection from lipotoxicity. JCI Insight 2017;2:e89160.
25. Du L, Lin L, Li Q, et al. IGF-2 Preprograms Maturing Macrophages to Acquire Oxidative Phosphorylation-Dependent Anti-inflammatory Properties. Cell Metab 2019;29:1363-1375.e8.
26. Maio N, Saneto RP, Steet R, et al. Disruption of cellular iron homeostasis by IREB2 missense variants causes severe neurodevelopmental delay, dystonia and seizures. Brain Commun 2022;4:fcac102.
27. Yang X, Feng H, Kim J, et al. PRR34-AS1 promotes mitochondrial division and glycolytic reprogramming in hepatocellular carcinoma cells through upregulation of MIEF2. Acta Biochim Biophys Sin (Shanghai) 2024. [Epub ahead of print]. doi: 10.3724/abbs.2024083.
28. Baran N, Lodi A, Dhungana Y, et al. Inhibition of mitochondrial complex I reverses NOTCH1-driven metabolic reprogramming in T-cell acute lymphoblastic leukemia. Nat Commun 2022;13:2801.
29. Wei Q, Chen L, Luo W, et al. PDE12 disrupts mitochondrial oxidative phosphorylation and mediates mitochondrial dysfunction to induce oral mucosal epithelial barrier damage in oral submucous fibrosis. Eur J Pharmacol 2024;967:176353.
30. Lone A, Harris RA, Singh O, et al. p66Shc activation promotes increased oxidative phosphorylation and renders CNS cells more vulnerable to amyloid beta toxicity. Sci Rep 2018;8:17081.
31. Codella R, Alves TC, Befroy DE, et al. Overexpression of UCP3 decreases mitochondrial efficiency in mouse skeletal muscle in vivo. FEBS Lett 2023;597:309-19.
32. Yi M, Li T, Niu M, et al. TGF-β: A novel predictor and target for anti-PD-1/PD-L1 therapy. Front Immunol 2022;13:1061394.
33. Aquila S, Santoro M, Caputo A, et al. The Tumor Suppressor PTEN as Molecular Switch Node Regulating Cell Metabolism and Autophagy: Implications in Immune System and Tumor Microenvironment. Cells 2020;9:1725.
34. Xu X, Zhang M, Xu F, et al. Wnt signaling in breast cancer: biological mechanisms, challenges and opportunities. Mol Cancer 2020;19:165.
35. Xia L, Oyang L, Lin J, et al. The cancer metabolic reprogramming and immune response. Mol Cancer 2021;20:28.
36. Zhou Y, Wang H, Luo Y, et al. Effect of metabolism on the immune microenvironment of breast cancer. Biochim Biophys Acta Rev Cancer 2023;1878:188861.
37. Choi H, Na KJ. Different Glucose Metabolic Features According to Cancer and Immune Cells in the Tumor Microenvironment. Front Oncol 2021;11:769393.
38. Loi S, Michiels S, Adams S, et al. The journey of tumor-infiltrating lymphocytes as a biomarker in breast cancer: clinical utility in an era of checkpoint inhibition. Ann Oncol 2021;32:1236-44.
39. Tower H, Ruppert M, Britt K. The Immune Microenvironment of Breast Cancer Progression. Cancers (Basel) 2019;11:1375.
40. Sivapalan L, Anagnostou V. Genetic variation in antigen presentation and cancer immunotherapy. Immunity 2022;55:3-6.
41. Mills CD, Ley K. M1 and M2 macrophages: the chicken and the egg of immunity. J Innate Immun 2014;6:716-26.
42. Cheng M, Chen Y, Xiao W, et al. NK cell-based immunotherapy for malignant diseases. Cell Mol Immunol 2013;10:230-52.
43. Ames E, Murphy WJ. Advantages and clinical applications of natural killer cells in cancer immunotherapy. Cancer Immunol Immunother 2014;63:21-8.

**Cite this article as:** Xia MZ, Dong SF, Wang CL. Oxidative phosphorylation-related genes for prognosis and tumor microenvironment in breast cancer. Transl Cancer Res 2025;14(1):497-511. doi: 10.21037/tcr-24-1181